Biophysical Chemistry 137 (2008) 81–87

Contents lists available at ScienceDirect

Biophysical Chemistry

journal homepage: http://www.elsevier.com/locate/biophyschem

Probing conformational changes in orphan nuclear receptor: The NGFI-B intermediate is a partially unfolded dimer

Wanius Garcia [1], Ana Carolina M. Figueira, Mario de Oliveira Neto, Carolina A. de Guzzi, Hilde H. Buzzá, Rodrigo V. Portugal, Marcos R. Calgaro, Igor Polikarpov *

Instituto de Física de São Carlos, Universidade de São Paulo, Av. Trabalhador Saocarlense 400, São Carlos, SP, 13560-970, Brazil

ARTICLE INFO

Article history:
Received 27 April 2008
Received in revised form 12 July 2008
Accepted 14 July 2008
Available online 18 July 2008

Keywords:
Orphan nuclear receptors
Conformational intermediate
Chemical unfolding
SAXS
Kratky plot

ABSTRACT

Human nerve growth factor-induced B (NGFI-B) is a member of the NR4A subfamily of orphan nuclear receptors (NRs). Lacking identified ligands, orphan NRs show particular co-regulator proteins binding properties, different from other NRs, and they might have a non-classical quaternary organization. A body of evidence suggests that NRs recognition of and binding to ligands, DNA, homo- and heterodimerization partners and co-regulator proteins involve significant conformational changes of the NR ligand-binding domains (LBDs). To shed light on largely unknown biophysical properties of NGFI-B, here we studied structural organization and unfolding properties of NGFI-B ligand (like)-binding domain induced by chemical perturbation. Our results show that NGFI-B LBD undergoes a two-state guanidine hydrochloride (GndHCl) induced denaturation, as judged by changes in the α-helical content of the protein monitored by circular dichroism spectroscopy (CD). In contrast, changes in the tertiary structure of NGFI-B LBD, reported by intrinsic fluorescence, reveal a clear intermediate state. Additionally, SAXS results demonstrate that the intermediate observed by intrinsic fluorescence is a partially folded homodimeric structure, which further unfolds without dissociation at higher GndHCl concentrations. This partially unfolded dimeric assembly of NGFI-B LBD might resemble an intermediate that this domain access momentarily in the native state upon interactions with functional partners.

1. Introduction

The nuclear receptors (NR) superfamily is comprised of proteins that have evolved to mediate a complex array of extracellular signals into transcriptional responses, regulating many biological processes, including cell growth, differentiation, metabolism, embryogenesis, and morphogenesis of higher organisms [1]. Most of the nuclear receptors reside within the cellular cytoplasm, and migrate to the nucleus to activate transcription of target genes in response to specific lipophilic ligands such as steroids, thyroid hormones, retinoids, vitamin D, prostaglandins, fatty acids, among others [2,3]. For approximately one-third of identified nuclear receptors no ligands have been identified to date, and hence they are referred to as orphan nuclear receptors [4]. Extensive research conducted in the last several years resulted in the identification of ligands for a handful of orphan nuclear receptors. However, the ligands for a number of orphan nuclear receptors are still unknown, or indeed do not exist [4].

Orphan nuclear receptor subfamily members share similar structural features within three major structural domains: the N-terminal domain, the most variable in size and sequence [4,5]; the centrally-located DNA-binding domain, which is the most conserved and confers the ability to recognize specific target DNA sequences [6]; and the C-terminal ligand (like)-binding domain, a multifunctional domain responsible for ligand-dependent transcriptional activation in liganded receptors, and that also plays a role in co-regulators recruitment [7].

In humans, the NR4A subfamily of orphan nuclear receptors (NRs) comprises three members: NGFI-B (NR4A1), also referred as NAK1, Nur77, ST-59, TR3 and eight other aliases [8]; NURR1 (NR4A2), and NOR1 (NR4A3). Monomeric, homodimeric, or heterodimeric NR4A receptors regulate target gene transcription from target sequences such as AAAGGTCA, termed NGFI-B response elements [9,10] in a cell type- and promoter-dependent manner [8,11–13]. In addition, NGFI-B and Nurr1 act on DR5 elements (AGGTCANNNAAAGGTCA) as heterodimers with RXR, a common dimerization partner of NRs [14,15], whereas NOR-1 fails to form stable RXR heterodimers [13]. In heterodimers, agonist-bound RXR contributes to transcriptional activation [11,12]. Members of this orphan receptors subgroup exhibit homologous DNA-binding domains, partially homologous ligand (like)-binding and transactivation domains [4].

All the NR4A receptors play important roles in the nervous, endocrine, and immune systems, and they are an immediate-early response gene products that are induced after stimulation with serum, growth factors, and nerve growth factor [16,17]. NGFI-B was originally

* Corresponding author. Tel.: +55 16 3373 8088; fax: +55 16 3373 9881.
E-mail address: ipolikarpov@if.sc.usp.br (I. Polikarpov).
[1] Present address: Laboratoire de Physique des Solides, Université Paris, Orsay, France.

0301-4622/$ – see front matter © 2008 Elsevier B.V. All rights reserved.
doi:10.1016/j.bpc.2008.07.005

identified by virtue of its rapid induction by serum in fibroblasts and by nerve growth factor (NGF) in cell line PC12 [16,17]. It is expressed in various tissues, notably the brain, and plays a role in multiple cellular events such as cell proliferation, differentiation and apoptosis [18,19]. The importance of NGFI-B in the apoptotic process was earlier demonstrated in knockout experiments in T-cell hybridomas [18,20]. In the thymus, NGFI-B acts upon the T lymphocytes in both pro-apoptotic [21] and anti-apoptotic manners [22]. However, it was recently shown that NGFI-B protein translocates to mitochondria to initiate the apoptotic process, a distinct function from that carried out by transcription factors [23]. Also, the receptor has been implicated in neurodegenerative pathologies, such as Parkinson disease, maniac depression, and schizophrenia [24].

The recent crystallographic structures of NURR1 and NGFI-B LBDs revealed that these receptors do not have a canonical ligand-binding pocket (LBP), with significant structural differences from the classical NR [25,26]. The LBD structure of these orphan receptors reveals a tight packing of side chains of several bulky hydrophobic residues in the LBP, normally occupied by ligands. Moreover, in contrast to what is generally observed in NR LBDs, in the orphan receptors NURR1 and NGFI-B, the co-activator cleft constituted by H3, H4, and H12 has a hydrophilic rather than a hydrophobic nature. These results are consistent with a notion that orphan receptors cannot be modulated by ligands. It was experimentally proved that a different co-regulator interface could be used by Nurr1 to modulate gene transcription [27]. Co-repressors, but not co-activators, were shown to be recruited by (apo) Nurr1 [27].

Surprisingly, however, Safe and coworkers recently demonstrated that 1,1-bis(3′indolyl)-1-(*p*-substituted phenyl)methanes containing trifluoromethyl, hydrogen, and methoxy substituents, induce NGFI-B-dependent transactivation in cancer cell lines through cellular apoptotic mechanisms. It was also demonstrated that the ligand binding was LBD-dependent, and it caused conformational changes in the receptor, leading to the steroid receptor co-activator 1 (SRC-1) recruitment [28]. The exact location of the ligand-binding site on the LBD structure and the nature of the conformational changes induced in NGFI-B LBD by ligand binding currently remain unknown.

Moreover, unexpected non-classical dimeric organization of the NGFI-B LBD has been reported recently, as revealed by small-angle X-ray scattering (SAXS) analysis and hydrogen/deuterium exchange (H/D-Ex) studies followed by mass spectrometry [29]. SAXS and H/D-Ex experiments revealed unexpected similarity between NGFI-B LBD and the alternative dimer interface observed in the crystallographic studies of glucocorticoid receptor (GR) [29,30], which might be responsible for the ability of GR to inhibit NGFI-B DNA-binding and NGFI-B-dependent transcription on a cellular level [30].

It is well accepted that NRs recognition of and binding to ligands, DNA, homo- and heterodimerization partners, and co-regulator proteins are mediated by pronounced conformational changes, particularly in their LBD region [7,15]. However, in contrast with the wealth of structural and functional information available for NRs, little is known about their conformational dynamics. It is clear, for example, that ligand binding provokes drastic changes in both position and orientation of the C-terminal helix 12 (H12), accompanied by conformational dynamics of the other parts of LBD. The same H12 is involved in the interaction with the co-regulator proteins and dimerization partners [7,31]. It was recently revealed that binding of co-activators to estrogen receptor (ER) induces novel markedly stabilized receptor conformation [32]. Furthermore, it was demonstrated that the ligand binding significantly increases ER thermal stability, the helical content of its LBD [33], and directly influences ER dimer affinity and dimer dissociation rates [34]. ER interactions with its cognate DNA response elements also markedly improve its conformational stability against temperature denaturation [35]. Finally, the group of Katzenellenbogen probed conformational dynamics of ER by GndHCl-induced unfolding followed by intrinsic tryptophan fluorescence [36]. It was demonstrated that moderate concentrations of GndHCl (c.a. 1.5 M) induce partially unfolded intermediate state of ER molecule, which is unable to bind ligand effectively. The authors argued that the observed partially unfolded state induced by GndHCl might involve H12 reorientation, and ligand-binding pocket opening, and may resemble an intermediate conformation that ER LBD accesses transiently under physiological conditions upon ligand binding or dissociation.

In this paper, we report the first studies of the conformational dynamics of NGFI-B LBD chemical unfolding monitored by a combination of intrinsic and extrinsic fluorescence, circular dichroism spectroscopy (CD), and small X-ray scattering (SAXS) measurements. Taken together, the results indicated the existence of an intermediate state present during the chemical unfolding of NGFI-B LBD. SAXS results indicated that the intermediate obtained with approximately 3 M of GndHCl at 20 °C is a partially folded structure. These biophysical studies can be expected to provide essential insights into the understanding of the conformational dynamics and stability of NGFI-B LBD, relevant to a series of important physiological and pathological processes.

2. Materials and methods

2.1. Materials

The bacterial expression vector pET28a(+) and Ni–NTA resin were purchased from Novagen. Guanidine hydrochloride (GndHCl), dithiothreitol (DTT), and 1-anilino-8-naphthalenesulfonic acid (ANS) were purchased from Sigma. All other chemical reagents used in this study were of analytical grade (Sigma, Amersham).

2.2. Expression and purification of the recombinant NGFI-B LBD

The expression and purification of the NGFI-B LBD were carried out as described previously [29]. After the purification, the final NGFI-B LBD was in buffer 10 mM Tris–HCl pH 8.0, containing 100 mM NaCl. The NGFI-B LBD concentration was determined from the UV absorbance at 280 nm using the theoretical extinction coefficient (15,845 M^{-1} cm^{-1}), based on its amino acid composition, using a U-2001 Hitachi spectrophotometer.

2.3. Circular dichroism spectroscopy (CD)

Chemical unfolding of NGFI-B LBD was monitored by far-UV CD spectroscopy using a J-715 Jasco spectropolarimeter equipped with a temperature control. CD spectra were measured from samples in 1.0 mm path length quartz cuvettes, and were the average of 16 accumulations, using a scanning speed of 100 nm min^{-1}, a spectral bandwidth of 1 nm, and a response time of 0.5 s. The NGFI-B LBD concentration was approximately 10 μM in buffer 10 mM Tris–HCl pH 8.0, containing 100 mM NaCl and 0.5 mM DTT. Chemical unfolding of NGFI-B LBD was characterized by measuring the ellipticity changes at 222 nm, at 20 °C, induced by the increases in GndHCl concentrations (0–6 M). CD spectra were obtained on a degree ellipticity scale. The ellipticity data obtained from the study of chemical unfolding were analyzed assuming that this is an irreversible transition process. The buffer contribution was subtracted in all of the experiments.

2.4. Fluorescence spectroscopy

NGFI-B LBD at 10 μM and different GdnHCl concentrations (0–6 M) were used in all experiments. All experiments were carried out at 20 °C, in buffer 10 mM Tris–HCl pH 8.0, containing 100 mM NaCl and 0.5 mM DTT in a steady-state spectrofluorimeter model K2 ISS, equipped with a refrigerated circulator. Intrinsic fluorescence spectra were obtained by excitation at 295 nm, and the emission spectra were

monitored from 300 to 450 nm. Relevant information about macromolecule conformational flexibility can be obtained by considering the fluorescence spectral center of mass [37,38]. In this case, the fluorescence spectral center of mass (λ_{cm}) was calculated, for each concentration of chaotropic agents, according to the equation [37,38]:

$$\lambda_{cm} = \frac{\sum \lambda I(\lambda)}{\sum I(\lambda)} \quad (1)$$

where λ is the emission wavelength, and $I(\lambda)$ represents the fluorescence intensity at wavelength λ. The buffer contribution was subtracted in all of the experiments.

2.5. ANS fluorescence assay

NGFI-B LBD at 10 μM and different GndHCl concentrations, varying from 0 to 6 M, in 10 mM Tris–HCl buffer, pH 8.0, containing 100 mM NaCl and 0.5 mM DTT were used in all experiments. For those experiments performed in the presence of ANS (50 μM), the excitation wavelength was set at 360 nm, and the emission spectra were collected from 400–600 nm. The intensity of the ANS interaction was monitored from the emission intensity measured at 464 nm (after subtraction of the buffer contribution), and determined as a function of the GdnHCl concentration. All experiments were carried out in triplicate at 20 °C.

2.6. Small-angle X-ray scattering (SAXS)

The NGFI-B LBD concentrations used for small-angle X-ray scattering (SAXS) measurements were approximately 5 mg/mL (200 μM) in 10 mM sodium phosphate buffer, pH 8.0, containing 100 mM NaCl, 1 mM DTT and different GndHCl concentrations (0–3 M). The samples were centrifuged for 15 min at 13.000 ×g (at 10 °C) prior to the SAXS measurements and the GndHCl addition. All data were collected on the SAXS synchrotron beamline at the LNLS (Campinas, Brazil) [39]. The wavelength of the incident monochromatic X-ray beam was $\lambda = 1.488$ Å. A 2D X-ray position sensitive detector was utilized to record the scattered intensity as a function of the modulus of the scattering vector q (here $q = 4 \cdot \pi \cdot \sin\theta/\lambda$, where θ is half the scattering angle). The parasitic scattering from air and beamline windows were subtracted from the total measured intensities. The sample-to-detector distance (1493.63 mm) was adjusted in order to record the scattering intensity for q values ranging from 0.10 to 2.26 nm^{-1}. The samples were loaded into cells made of two thin parallel mica windows, and the cell was kept at 20 °C during the measurements. Data analysis was performed using the GNOM program [40,41].

3. Results and discussion

In this study, the unfolding transition and stability of the recombinant NGFI-B LBD were investigated using several biophysical techniques as CD spectroscopy, intrinsic and extrinsic fluorescence spectroscopy and small-angle X-ray scattering (SAXS). The secondary structure stability of the recombinant NGFI-B LBD, in the presence of GdnHCl, was studied by far-UV CD. Fig. 1A shows the CD spectra of NGFI-B LBD at 20 °C (pH 8.0) in different GndHCl concentrations (0, 2.5, 3.75 and 6 M). The CD spectrum of NGFI-B LBD at 20 °C and 0 M GndHCl exhibits two negative minimums at approximately 222 and 208 nm, indicating a substantial amount of α-helical structure (Fig. 1A, solid line). Probing α-helical content of the protein at 222 nm (Fig. 1B), we observed a loss of secondary structure with the increase in the GndHCl concentrations, suggesting a loss of NGFI-B α-helical content. Fitting the data (Fig. 1B) resulted in a denaturant concentration, [GndHCl], equal to 3.2 ± 0.1 M at the middle of transition. These results suggest that there are no intermediates present in detectable amounts during the chemical

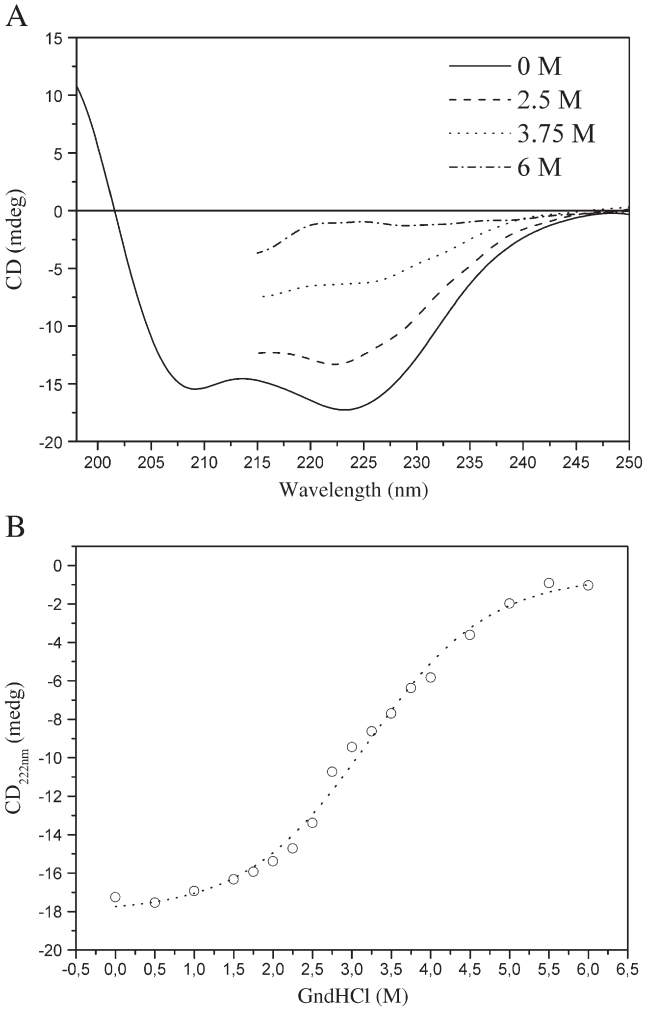

Fig. 1. Chemical unfolding monitored by CD. (A) Effects of GndHCl-induced denatured on the secondary structure of NGFI-B LBD at 20 °C monitored by far-UV CD spectroscopy. Due to the increased absorption of GndHCl at lower wavelengths several spectra are limited due to the poor signal-to-noise ratio. (B) CD data were monitored at 222 nm as a function of GndHCl concentration (0–6 M).

unfolding transition monitored by CD. In addition, NGFI-B LBD can be completely unfolded by treatment with 6 M GdnHCl at room temperature (Fig. 1A, dash–dot line). The refolding of the recombinant NGFI-B LBD revealed that the chemical unfolding by GndHCl was irreversible (data not shown).

To examine in more detail this apparent two-state transition of the protein secondary structure, we analyzed changes in the fluorescence emission using the same chemical denaturation protocol. Thus, chemical unfolding of NGFI-B LBD was studied by intrinsic fluorescence spectroscopy at 20 °C. Fig. 2A shows the fluorescence spectra of the recombinant NGFI-B LBD in different GndHCl concentrations (0, 2.5, 4.5 and 6 M). The presence of two tryptophan residues, W419 and W481, in the recombinant NGFI-B LBD allowed us to follow the unfolding transition. The tryptophan residues W419 and W481 are located, respectively, at the C-terminal part of helix 3 and the N-terminal part of helix 5 of the LBD, and they are buried within the protein matrix (Fig. 2B). Since aromatic residues, tryptophans in this case, are extremely sensitive to the polarity of their immediate environment, changes in the center of mass of the fluorescence signal reflect conformational changes induced in the protein [37,38]. The spectral center of mass (λ_{cm}) of each emission spectrum as a function of GndHCl concentration (0–6 M) is shown in Fig. 2C. The changes in the tertiary structure of NGFI-B LBD as a function of GndHCl

concentration reported by the intrinsic fluorescence emission (Figs. 2 and 3) do not coincide with the CD spectroscopy data.

The intrinsic fluorescence data show that the recombinant NGFI-B LBD has an emission peak at approximately 334 nm, suggesting that, on average, its two tryptophan residues are buried inside of a solvent

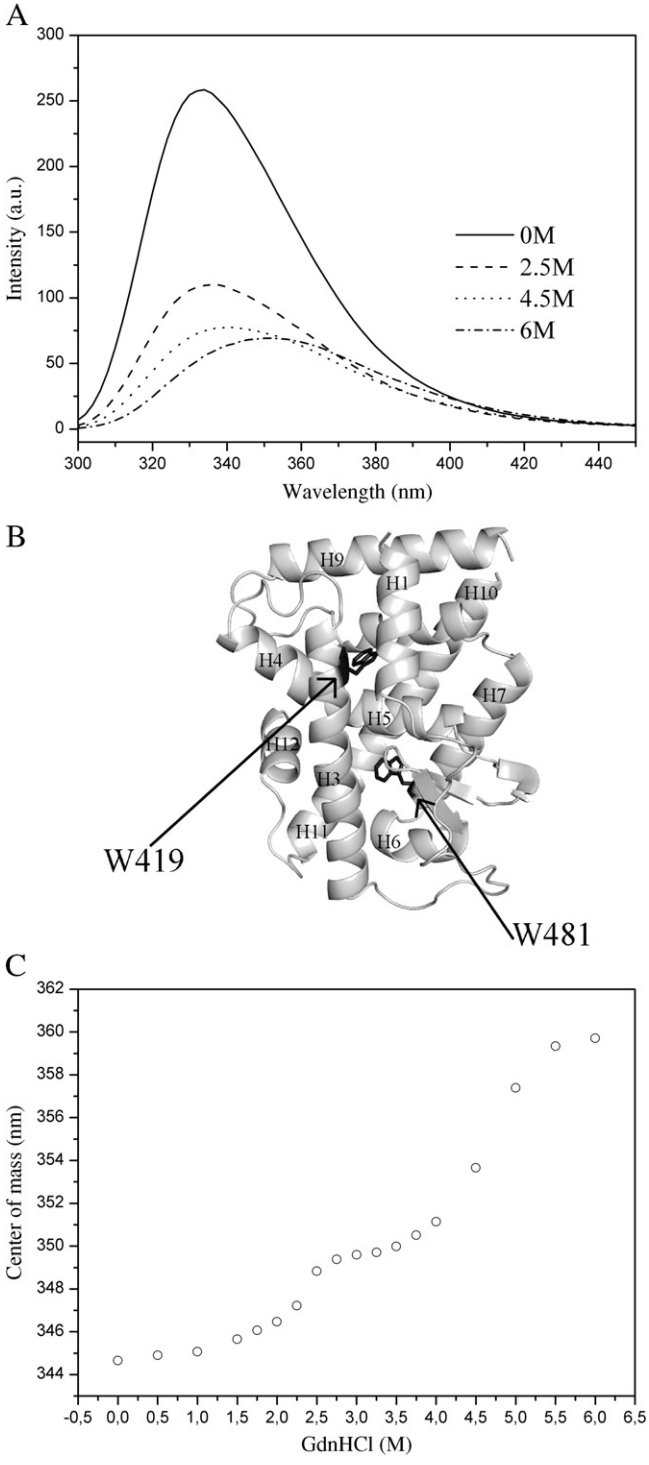

Fig. 2. Chemical unfolding monitored by fluorescence. (A) Effects of GndHCl-induced unfolding on the tertiary structure of NGFI-B ligand (like) binding domain. NGFI-B LBD samples were exposed to 0–6 M GndHCl at 20 °C. Solid line in the figure correspond the NGFI-B LBD in 0 M GndHCl. Excitation wavelength was 295 nm and emission was collected from 300 nm to 450 nm. (B) The NGFI-B LBD structure with its two tryptophans (W419 and W 481) shown in black, and indicated by arrows. W419 is located at the C-terminal part of helix 3 (H3) whereas W481 is in the N-terminal part of helix 7 (H7). (C) Spectral center of mass as a function of GndHCl concentration.

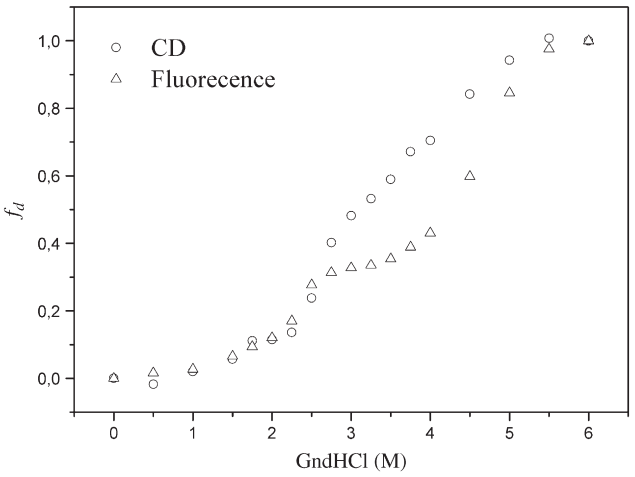

Fig. 3. CD and fluorescence spectroscopy. Comparison between CD and fluorescence spectroscopy measurements.

inaccessible protein core (Fig. 2A). However, the incubation of the protein with increasing amounts of GndHCl resulted in a significant shift in the center of mass [37,38] and a bathochromic red shift in the fluorescence emission maximum (from 334 nm to 360 nm), and also in a severe quenching of the fluorescence emission intensity (Fig. 2A and C). In contrast with the CD results, the GndHCl-induced unfolding as monitored by the intrinsic fluorescence unambiguously reveals an intermediate state at the GndHCl concentrations around 2.75 M and 3.5 M (Fig. 3). An abrupt loss of tertiary structure is observed above 3.5 M of the denaturing agent. Finally, the fluorescence emission spectra of NGFI-B LBD at high GndHCl concentrations (5 to 6 M) suggest that both tryptophan residues are highly exposed to the aqueous environment (maximum red shift of ~360 nm), characteristic of a completely unfolded protein. Again, the chemical refolding of NGFI-B LBD studies by fluorescence emission appeared to be an irreversible process (data not shown).

The fluorescence data therefore clearly reveal aspects of the chemical denaturation of NGFI-B LBD which are not evident from the CD data. Structural alterations of the molecule begin to occur at much lower GndHCl concentrations. However, between 2.75 M and 3.5 M GndHCl concentrations, alterations in the secondary structure occur whilst retaining both tryptophans buried within the hydrophobic core. The fluorescence data readily permit the identification of an intermediate along the unfolding pathway, which is not observable by CD spectroscopy. The reduction in the intensity of the negative CD signal at 222 nm suggests that this intermediate has a lower relative α-helical content than the native structure.

To better characterize the nature of the conformational intermediate observed by intrinsic fluorescence in terms of hydrophobic surface exposure, we used the extrinsic fluorescence marker, ANS, for probing of exposed hydrophobic areas of the chemically induced denaturation of NGFI-B LBD (Fig. 4). The fluorescence probe ANS binds non-covalently to hydrophobic surfaces in partially folded intermediates with much higher affinity than to native or completely unfolded proteins [42,43], resulting in a marked increased in the fluorescence emission when compared with the emission of free ANS in aqueous solution. Fig. 4A shows ANS spectra in the presence of NGFI-B LBD and several GndHCl concentrations (0, 1.5, 3 and 6 M). As can be seen in Fig. 4A (solid line), ANS shows a detectible affinity for the protein even in the absence of GndHCl, indicating the presence of exposed hydrophobic regions on the native structure. This rises significantly within a relatively narrow concentration range presenting a maximum increase of approximately threefold, corresponding to a GdnHCl concentration of 1.5 M, and indicating increased exposure of additional hydrophobic regions in the protein as a consequence of

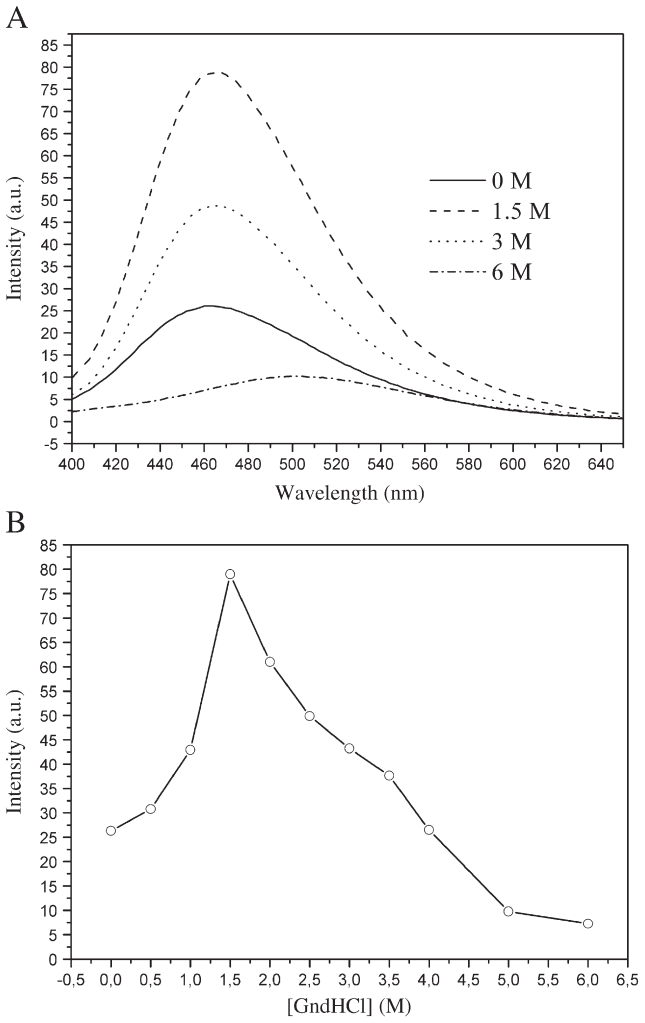

Fig. 4. ANS fluorescence assay. (A) ANS fluorescence emission spectra in the presence of NGFI-B LBD at different GndHCl concentrations. An increase significant in the capacity to bind ANS was observed at 1.5 M GndHCl, suggesting the exposure of hydrophobic regions in the NGFI-B LBD. (B) Emission intensity at 464 nm as a function of GndHCl concentration.

chemical unfolding. At GndHCl concentrations above 1.5 M a marked decay of the fluorescence signal is observed and, as expected, the partially folded structure observed between 2.75 M and 3.5 M GndHCl no longer exhibits hydrophobic patches exposed to the solvent, as judged by the loss of ANS binding (Fig. 4B). The addition of 5 M–6 M GndHCl completely abolished the binding of ANS to NGFI-B LBD (Fig. 4A and B).

Taken together, all data permit us to infer that the transition from the native state to that of the intermediate involves alterations at both secondary and tertiary structural levels. An apparent loss of α-helical content is accompanied by an increase in the exposed hydrophobic surface whilst simultaneously retaining the burial of both tryptophan residues within the hydrophobic core.

SAXS is a technique applicable to the analysis of the global shapes, dimensions and oligomeric states of macromolecules in solution. The X-ray scattering curves for NGFI-B LBD in the presence of 0 M, 1 M and 3 M GndHCl concentrations were acquired. The X-ray scattering data collected from the native protein samples are consistent with the non-classical NGFI-B LBD homodimer observed in our previous experiments [29]. SAXS measurements in the presence of high concentrations of GdnHCl (>3 M) were not possible due to the high X-ray absorption by the GndHCl molecules in the solvent. In Fig. 5A, the curves corresponding to the native protein, after subtraction of the buffer scattering, are shown together with those of the samples containing 1 M and 3 M urea within the q range up to 0.25 nm^{-1}. The raw scattering data clearly show that there are structural alterations of the molecule at both 1 M and 3 M GndHCl, as compared with the native one. In particular, the scattering curve measured in the presence of 3 M GndHCl is given as it corresponds to conditions where the plateau is observed in the intrinsic fluorescence experiments and therefore to an intermediate (Fig. 2C). In the presence of denaturant, the quality of the scattering curves limited the usable data to less than 1.5 nm^{-1}.

For a more sensitive analysis of the effects of GndHCl on the global compactness of NGFI-B LBD, the SAXS data have been analyzed in terms of the Kratky plot [44]. The Kratky plot, in Fig. 5B, aids in the structural interpretation of such alterations. For a system with a compact shape, this plot shows a well defined curve with an initial rising portion followed by a marked descent thereby forming a well defined maximum [45,46]. Nevertheless, the expected curve for a polymer in an extended or random coil conformation rises to a characteristic plateau, with no well defined maximum [47,48].

As can be seen in Fig. 5B both curves corresponding to measurements made in the absence of GndHCl (the native structure), and in the presence of 1 M GndHCl, show the well defined maxima expected for compact structures. However, in the case of the intermediate (3 M)

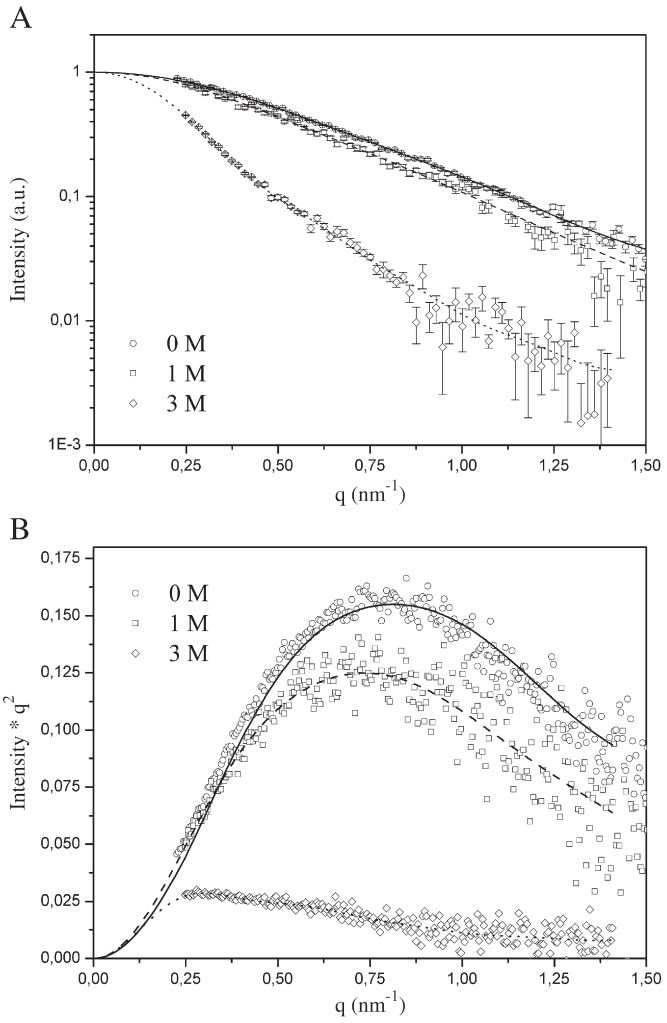

Fig. 5. Experimental solution scattering curves. (A) SAXS curves from NGFI-B LBD shown as the logarithm of the scattering intensity (log I) *versus* the momentum transfer q scale. The desmeared experimental curves (open points) denote the SAXS data and the error bars indicate the standard uncertainty in the measurement, native NGFI-B (○), 1 M GndHCl ( ) and 3 M GndHCl (◊). The solid curves correspond to the fit produced by GNOM. (B) Kratky plots for NGFI-B LBD following the same symbol convention as in (A).

the Kratky plot indicates an alteration both in the peak intensity and its position indicating that alterations to the compactness of the structure have occurred. This behavior is typically exhibited by elongated chains [45,46], indicating that in the presence of 3 M GndHCl NGFI-B LBD is unfolded, different to that observed for the native species. The maximum dimension of this dimer (as determined from the pair-distribution function) is 10 nm, which is consistent with the open NGFI-B homodimer mediated by a novel, non-canonical dimerization interface [29]. The intermediate, on the other hand, has a larger maximum dimension than the native structure (20 nm). The radii of gyration (R_g) for NGFI-B LBD in its native state, and in the presence of 3 M GndHCl, show an increase in this parameter, from 2.99 nm to 7.34 nm.

Furthermore, from the dimensions of the particle it is clear that the concentrations of GndHCl necessary to induce the intermediate formation do not lead to the dissociation of the dimer. This fact is also consistent with the native gel electrophoresis experiments, which show that NGFI-B dimers are the predominant species at all concentrations of GndHCl used in the assays (0 to 3 M) (data not shown). In the presence of 3 M GndHCl, the Kratky plot displays not well defined peak, indicating that NGFI-B LBD has largely lost its compact core (Fig. 5B). This is consistent with both fluorescence and ANS fluorescence data, which indicate that under these conditions, the protein is denatured but both tryptophan residues remain partially buried.

In conclusion, the unfolding behavior of NGFI-B LBD in GndHCl was found to be a two-step process at pH 8.0 and 20 °C. The first step led to the formation of an intermediate conformation, followed by a second step that was due to the unfolding of the intermediate state. This intermediate presents the following characteristics: 1) it has reduced secondary structure content, 2) it has largely lost its compact core, 3) it does not exhibit hydrophobic patches exposed to the solvent and 4) it retains its native tertiary structure in which both tryptophan residues remain partially buried inside the hydrophobic core. Moreover, quaternary structure of the NGFI-B non-canonical "open" dimer is maintained in the intermediate state induced by GndHCl. This fact clearly indicates that the observed non-classical dimerization interface is very resistant toward chemical perturbations, and indicates an importance of this quaternary structure architecture for the homodimerization of NGFI-B in solution. Fig. 6 summarizes schematically the different conformational states described in this study.

Our experimental study reveals that similarly to estrogen receptor, the orphan nuclear receptor NGFI-B forms partially folded intermediate state induced by denaturant. Both ER and NGFI-B exhibit increased exposure of hydrophobic regions of the LBDs at GndHCl concentrations close to 1.5 M. In structural terms, this may be related to the repositioning of the C-terminal H12, and partial destabilization of the parts of the LBDs with the simultaneous exposure of the hydrophobic regions of the protein to the aqueous environment. The repositioning of H12 regulates accessibility of a hydrophobic cleft formed by parts of helices 3, 4, 5, and 12, which assemble a docking site for the LXXLL sequence motif found in various co-regulator proteins [47–49]. Although it is believed that in non-liganded ER the H12 is in an open conformation [50], whereas in the crystal structure of the orphan NR NGFI-B it seals the entrance of the LBD [26], mild denaturing conditions have very similar effect on these two proteins. The reason might be the fact that in solution H12 is in fact in the dynamic equilibrium between "open" and "close" conformations, which seems to be shifted toward more "hydrophobically exposed" state of the LBD by the influence of GndHCl. These observations find support in the biophysical and computational studies of another nuclear receptor. Our preliminary studies of urea-induced denaturation of thyroid hormone nuclear receptor ligand-binding domain (TR LBD) show that this nuclear receptor also loses a significant portion of the secondary structure elements, and its denaturation involves the formation of an intermediate state at the relatively low denaturant concentrations (approximately 1.5 M of urea, data not shown). Although the intermediate has a reduced α-helical content, it preserves both tertiary and quaternary structures. Furthermore, our molecular dynamics simulations of the temperature-induced denaturation of TR LBD reveal that denaturing of the receptor starts with the graduate decrease of the α-helical content of the protein, beginning with the C-terminal helix 12, and progresses to a very significant lost of the secondary structure without affecting overall compactness of the protein. Finally, the protein denatures, losing both secondary and tertiary structures (unpublished results). These observations indicate that NR LBD denaturation, which begins by the graduate lost of the alpha helical content at relatively mild denaturation conditions, and involves formation of a partially melted intermediate, might be common for a number of nuclear receptors. This behavior seems to be directly related to NRs structural organization, which involves a loosely folded and conformationally flexible C-terminal alpha helix H12, important for NR function.

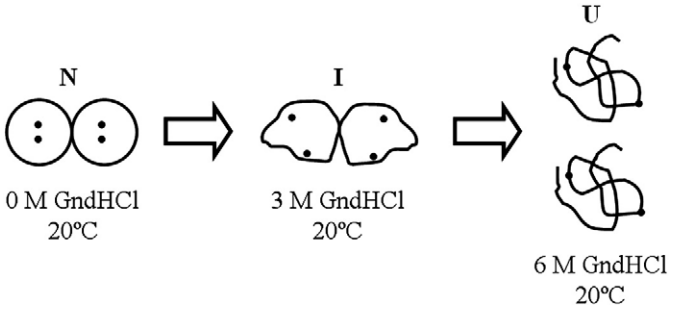

Fig. 6. Reaction scheme for NGFI-B LBD unfolding. N, I and U indicate the native form, intermediate state and unfolded form of NGFI-B LBD, respectively. The symbol ● indicates tryptophan residues.

It is obvious that not every NR follows this scenario in all details. For example, there are several differences in the conformational dynamics between NGFI-B and ER. ER LBD undergoes two-state transition from native into denatured state (for apo-ERα LBD the middle of transition corresponds to 1.5 M GndHCl [36]), whereas NGFI-B LBD unfolds through the intermediate state observed at higher GndHCl concentrations (approximately 3 M). This orphan receptor intermediate still preserves part of its secondary structure, retains it tertiary structure, and does not present anymore-exposed hydrophobic regions. We argue that some of these differences could be directly related to the fact that the ligand-binding (like) pocket of the orphan NR is occupied by bulky hydrophobic side chains, and does not contain a cavity which would accommodate ligand in the NRs capable of ligand binding. Ligand-binding and co-regulators recruitment must occur differently in the NGFI-B, and perhaps other orphan NR of the same family, as judged by the absence of internal volume in the native structure sufficient for ligand docking, and also by the novel quaternary organization, which permits an access to the alternative co-regulator-binding sites [51]. By analogy with the ER [36], it is tempting to speculate that the observed intermediate is directly related to the NGFI-B LBD transitional state, temporarily accessed by the orphan nuclear receptor under native conditions upon interactions with the co-regulator proteins and, perhaps, ligands. This argument is supported by the fact that the observed intermediate retains its quaternary structure as non-classical "open" dimer conformation which seems to be necessary for interactions with the widely spaced NGFI-B response elements [29,30].

Further studies are required to elucidate fine structural details of the NGFI-B LBD partially unfolded intermediate observed by fluorescence spectroscopy. It is clear, however, that better understanding of the conformational dynamics and biophysical characteristics of NGFI-B LBD are important to a deeper appreciation of orphan nuclear receptor activities at the molecular level.

Acknowledgements

The authors thank FAPESP for financial support via grants #06/00182-8, #02/14041-6 and 03/09462-5. We also thank Laboratório Nacional de Luz Síncrotron (LNLS) for the access to SAXS beamline and other facilities.

References

[1] A. Aranda, A. Pascual, Nuclear hormone receptors and gene expression, Physiological Reviews 81 (2001) 1269–1304.
[2] R.C.J. Ribeiro, P.J. Kushner, J.D. Baxter, The nuclear hormone receptor gene superfamily, Annual Review of Medicine 46 (1995) 443–453.
[3] R.C.J. Ribeiro, J.W. Apriletti, R.L. Wagner, W. Feng, P.J. Kushner, S. Nilsson, T.S. Scanlan, B.L. West, R.J. Fletterick, J.D. Baxter, X-ray crystallographic and functional studies of thyroid hormone receptor, Journal of Steroid Biochemistry and Molecular Biology 65 (1998) 133–141.
[4] V. Giguere, Orphan nuclear receptors: from gene to function, Endocrine Reviews 20 (1990) 689–725.
[5] V. Laydet, Evolution of the nuclear receptor superfamily: early diversification from an ancestral orphan receptor, Journal of Molecular Endocrinology 19 (1997) 207–226.
[6] M.S. Lee, S.A. Kliewer, J. Provencal, P.E. Wright, R.M. Evans, Structure of the retinoid X receptor alpha DNA binding domain: a helix required for homodimeric DNA binding, Science 260 (1993) 1117–1121.
[7] J.M. Wurtz, W. Bourguet, J.P. Renaud, V. Vivat, P. Chambon, D. Moras, H. Gronemeyer, A canonical structure for the ligand-binding domain of nuclear receptors, Nature Structural Biology 3 (1996) 87–94.
[8] R.F. Paulsen, K. Granas, H. Johnsen, V. Rolseth, S. Sterri, Three related brain nuclear receptors, NGFI-B, Nurr1, and NOR-1, as transcriptional activators, Journal of Molecular Neuroscience 6 (1995) 249–255.
[9] T.E. Wilson, T.J. Fahrner, J. Milbrandt, The orphan receptors NGFI-B and steroidogenic factor 1 establish monomer binding as a third paradigm of nuclear receptor–DNA interaction, Molecular and Cellular Biology 13 (1993) 5794–5804.
[10] M. Maira, C. Martens, A. Philips, J. Drouin, Heterodimerization between members of the Nur subfamily of orphan nuclear receptors as a novel mechanism for gene activation, Molecular and Cellular Biology 19 (1999) 7549–7557.
[11] K. Maruyama, T. Tsukada, N. Ohkura, S. Bandoh, T. Hosono, K. Yamaguchi, The NGFI-B subfamily of the nuclear receptor superfamily, International Journal of Oncology 12 (1998) 1237–1243.
[12] S.W. Law, O.M. Conneely, F.J. DeMayo, B.W. O'Malley, Identification of a new brain-specific transcription factor, NURR1, Molecular Endocrinology 6 (1992) 2129–2135.
[13] D.S. Castro, M. Arvidsson, B.M. Bondesson, T. Perlmann, Activity of the Nurr1 carboxyl-terminal domain depends on cell type and integrity of the activation function 2, Journal Biological Chemistry 274 (1999) 37483–37490.
[14] B.M. Forman, K. Umesono, J. Chen, R.M. Evans, Unique response pathways are established by allosteric interactions among nuclear hormone receptors, Cell 81 (1995) 541–550.
[15] T. Perlmann, L. Jansson, A novel pathway for vitamin A signaling mediated by RXR heterodimerization with NGFI-B and NURR1, Genes & Development 9 (1995) 769–782.
[16] J. Milbrandt, J., Nerve growth-factor induces a gene homologous to the glucocorticoid receptor gene, Neuron 1 (1988) 183–188.
[17] T.G. Hazel, D. Nathans, L.F. Lau, A gene inducible by serum growth factors encodes a member of the steroid and thyroid hormone receptor superfamily, Proceedings of the National Academy Sciences of the United States of America 85 (1988) 8444–8448.
[18] Z.G. Liu, S.W. Smith, K.A. McLaughlin, L.M. Schwartz, B.A. Osborne, Apoptotic signals delivered through the t-cell receptor of a t-cell hybrid require the immediate-early gene nur77, Nature 367 (1994) 281–284.
[19] Y.M. He, Orphan nuclear receptors in T lymphocyte development, Journal of Leukocyte Biology 72 (2002) 440–446.
[20] J.D. Woronicz, B. Calnan, V. Ngo, A. Winoto, Requirement for the orphan steroid-receptor nur77 in apoptosis of t-cell hybridomas, Nature 367 (1994) 277–281.
[21] H.D. Youn, L. Sun, R. Prywes, J.O. Liu, Interleukin-1 receptor antagonist gene polymorphisms in carotid atherosclerosis, Science 22 (1999) 790–793.
[22] S. Suzuki, L.F. Chuang, R.H. Doi, R.Y. Chuang, Morphine suppresses lymphocyte apoptosis by blocking p53-mediated death signaling, Biochemical and Biophysical Research Communications 5 (2003) 802–808.
[23] H. Li, S.K. Kolluri, J. Gu, M.I. Dawson, X. Cao, P.D. Hobbs, B. Lin, G. Chen, J. Lu, F. Lin, Z. Xie, J.A. Fontana, J.C. Reed, X. Zhang, Cytochrome *c* release and apoptosis induced by mitochondrial targeting of nuclear orphan receptor TR3, Science 289 (2000) 1159–1164.
[24] I. Ethier, G. Beaudry, M. St-Hilaire, J. Milbrandt, C. Rouillard, D. Levesque, The transcription factor NGFI-B (Nur77) and retinoids play a critical role in acute neuroleptic-induced extrapyramidal effect and striatal neuropeptide gene expression, Neuropsychopharmacology 29 (2004) 335–346.
[25] Z. Wang, G. Benoit, J. Liu, S. Prasad, P. Aarnisalo, X. Liu, H. Xu, N.P.C. Walker, T. Perlmann, Structure and function of Nurr1 identifies a class of ligand-independend nuclear receptors, Nature 423 (2003) 555–560.
[26] R. Flaig, H. Greschik, C. Peluso-Iltis, D. Moras, Structural basis for the cell-specific activities of the NGFI-B and the Nurr1 ligand-binding domain, Journal of Biological Chemistry 280 (2005) 19250–19258.
[27] A. Codina, G. Benoit, J.T. Gooch, D. Neuhaus, T. Perlmann, J.W. Schwabe, Identification of a novel co-regulator interaction surface on the ligand binding domain of Nurr1 using NMR footprinting, Journal of Biological Chemistry 279 (2004) 53338–53345.
[28] S. Chintharlapalli, R. Burghardt, S. Papineni, S. Ramaiah, S. Yoon, S. Safe, Activation of Nur77 by selected 1,1-Bis(3′-indolyl)-1-(*p*-substituted phenyl)methanes induces apoptosis through nuclear pathways, Journal of Biological Chemistry 280 (2005) 24903–24914.
[29] M.R. Calgaro, M. Oliveira Neto, A.C.M. Figueira, M.A.M. Santos, R.V. Portugal, C.A. Guzzi, D.M. Saidemberg, L. Bleicher, J. Vernal, P. Fernandez, H. Terenzi, M.S.P. Palma, I. Polikarpov, Orphan nuclear receptor NGFI-B forms dimers with non-classical interface, Protein Science 16 (2007) 1762–1772.
[30] A. Philips, M. Maira, A. Mullick, M. Chamberland, S. Lesage, P. Hugo, J. Drouin, Antagonism between Nur77 and glucocorticoid receptor for control of transcription, Molecular and Cellular Biology 17 (1997) 5952–5959.
[31] J.P. Renauld, D. Moras, Structural studies on nuclear receptors, Cellular and Molecular Life Sciences 57 (2000) 1748–1769.
[32] A. Tamrazi, K.E. Carlson, A.L. Rodriguez, J.A. Katzenellenbogen, Coactivator proteins as determinants of estrogen receptor structure and function: spectroscopic evidence for a novel coactivator-stabilized receptor conformation, Molecular Endocrinology 19 (2005) 1516–1528.
[33] N. Greenfield, V. Vijayanathan, T.J. Thomas, M.A. Gallo, T. Thomas, Increase in the stability and helical content of estrogen receptor R in the presence of the estrogen response element: analysis by circular dichroism spectroscopy, Biochemistry 40 (2001) 6646–6652.
[34] A. Tamrazi, K.E. Carlson, J.R. Daniels, K.M. Hurth, J.A. Katzenellenbogen, Estrogen receptor dimerization: ligand binding regulates dimer affinity and dimer dissociation rate, Molecular Endocrinology 16 (12) (2002) 2706–2719.
[35] S.K. Nair, T.J. Thomas, N.J. Greenfield, A. Chen, H. He, T. Thomas, Conformational dynamics of estrogen receptors ERa and ERb as revealed by intrinsic tryptophan fluorescence and circular dichroism, Journal of Molecular Endocrinology 35 (2005) 211–223.
[36] A.C. Gee, J.A. Katzenellenbogen, Probing conformational changes in the estrogen receptor: evidence for a partially unfolded intermediate facilitating ligand binding and release, Molecular Endocrinology 15 (2001) 421–428.
[37] M.G. Botelho, M. Gralle, C.L.P. Oliveira, I. Torriani, S.T. Ferreira, Folding and stability of the extracellular domain of the human amyloid precursor protein, Journal of Biological Chemistry 278, 36 (2003) 34259–34267.
[38] C.F.S. Bonafé, C.M.R. Vital, R.C.B. Telles, M.C. Gonçalves, M.S.A. Matsuura, F.B.T. Pessine, D.R.C. Freitas, J. Vega, Tobacco mosaic virus disassembly by high hydrostatic pressure in combination with urea and low temperature, Biochemistry 37 (1998) 11097–11105.
[39] G. Kellermann, F. Vicentin, E. Tamura, M. Rocha, H. Tolentino, A. Barbosa, A. Craievich, I. Torriani, The small-angle X-ray scattering beamline of the Brazilian Synchrotron Light Laboratory, Journal of Applied Crystallography 30 (1997) 880–883.
[40] D.I. Svergun, A.V. Semenyuk, L.A. Feigin, Small-angle-scattering-data treatment by the regularization method, Acta Crystallographica 44 (1998) 244–250.
[41] D.I. Svergun, Determination of the regularization parameter in indirect-transform methods using perceptual criteria, Journal of Applied Crystallography 25 (1992) 495–503.
[42] S. Srisailam, H.M. Wang, T.K.S. Kumar, D. Rajalingam, V. Sivaraja, H.S. Sheu, Y.C. Chang, C. Yu, Amyloid-like fibril formation in an all beta-barrel protein involves the formation of partially structured intermediate(s), Journal of Biological Chemistry 277 (2002) 19027–19036.
[43] G.V. Semisotnov, N.A. Rodionova, V.P. Kutyshenko, B. Ebert, J. Blanck, O.B. Ptitsyn, Sequential mechanism of refolding of carbonic anhydrase-b, FEBS Letter 224 (1987) 9–13.
[44] S. Doniach, J. Bascle, T. Garel, H. Orland, Partially folded states of proteins—characterization by X-ray-scattering, Journal of Molecular Biology 254 (1995) 960–967.
[45] O. Glatter, O. Krakty, Small Angle X-ray Scattering, Academic Press Inc., New York, 1982.
[46] G.V. Semisotnov, H. Kihara, N.V. Kotova, K. Kimura, Y. Amemiya, K. Wakabayashi, I.N. Serdyuk, A.A. Timchenko, K. Chiba, K. Nikaido, T. Ikura, K. Kuwajima, Protein globularization during folding: a study by synchrotron small-angle X-ray scattering, Journal of Molecular Biology 262 (1996) 559–574.
[47] B.D. Darimont, R.L. Wagner, J.W. Apriletti, M.R. Stallcup, P.J. Kushner, J.D. Baxter, R.J. Fletterick, K.R. Yamamoto, Structure and specificity of nuclear receptor–coactivator interactions, Genes Development 12 (1998) 3343–3356.
[48] W. Feng, R.C.J. Ribeiro, R.L. Wagner, H. Nguyen, J.W. Apriletti, R.J. Fletterick, J.D. Baxter, P.J. Kushner, B.L. West, Hormone-dependent coactivator binding to a hydrophobic cleft on nuclear receptors, Science 280 (1998) 1747–1749.
[49] D.M. Heery, E. Kalkhoven, S. Hoare, M.G. Parker, A signature motif in transcriptional co-activators mediates binding to nuclear receptors, Nature 387 (1997) 733.
[50] M. Ruff, M. Gangloff, J.M. Wurtz, D. Moras, Estrogen receptor transcription and transactivation: structure–function relationship in DNA- and ligand-binding domains of estrogen receptors, Breast Cancer Research 2 (2000) 353–359.
[51] K.W. Nettles, G.L. Greene, Ligand control of coregulator recruitment to nuclear receptors, Annual Review of Physiology 67 (2005) 309–333.